ACS APPLIED MATERIALS & INTERFACES

Research Article

www.acsami.org

Synthesis of Fluorophore-Doped Polystyrene Microspheres: Seed Material for Airflow Sensing

Christopher J. Wohl,*[,†] Jacob M. Kiefer,[‡] Brian J. Petrosky,[§] Pacita I. Tiemsin,[†] K. Todd Lowe,[§] Pietro M. F. Maisto,[§] and Paul M. Danehy[†]

[†]NASA Langley Research Center, Hampton, Virginia 23681, United States

[‡]NASA Langley Research Summer Scholars (LARSS), NASA Langley Research Center, Hampton, Virginia 23681, United States

[§]Department of Aerospace and Ocean Engineering, Virginia Polytechnic Institute and State University, Blacksburg, Virginia 24060, United States

Supporting Information

ABSTRACT: Kiton red 620 (KR620) doped polystyrene latex microspheres (PSLs) were synthesized via soap-free emulsion polymerization to be utilized as a relatively nontoxic, fluorescent seed material for airflow characterization experiments. Poly(styrene-*co*-styrenesulfonate) was used as the PSL matrix to promote KR620 incorporation. Additionally, a bicarbonate buffer and poly(diallyldimethylammonium chloride), polyD, cationic polymer were added to the reaction solution to stabilize the pH and potentially influence the electrostatic interactions between the PSLs and dye molecules. A design of experiments (DOE) approach was used to efficiently investigate the variation of these materials. Using a 4-factor, 2-level response surface design with a center point, a series of experiments were performed to determine the dependence of these factors on particle diameter, diameter size distribution, fluorescent emission intensity, and KR620 retention. Using statistical analysis, the factors and factor interactions that most significantly affect the outputs were identified. These particles enabled velocity measurements to be made much closer to walls and surfaces than previously. Based on these results, KR620-doped PSLs may be utilized to simultaneously measure the velocity and mixing concentration, among other airflow parameters, in complex flows.

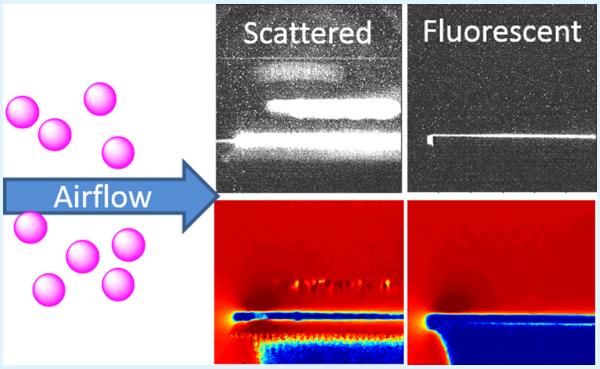

KEYWORDS: *kiton red 620, PSLs, particle image velocimetry (PIV), emulsifier-free emulsion polymerization, design of experiments, fluorescent particles*

1. INTRODUCTION

Microparticles are commonly used as a seed material in wind tunnel testing to measure airflow velocity. Two common measurement techniques include particle image velocimetry (PIV) and laser Doppler velocimetry (LDV).[1,2] In both techniques, a laser irradiates particles seeded in the flow. The particles then elastically scatter the light. In PIV, a camera takes pictures of an area of a flow field illuminated by a pulsed laser. The position of the seed particles in sequential images is used to determine velocities, enabling planar data analysis of turbulence levels, length scales, coherent flow structures, flow-induced forces, and moments. In LDV, two laser beams cross and interfere to create a fringe pattern which is used to determine point-wise velocities from the frequency of light scattered by the particles.[3]

Good seed materials for PIV and LDV must have a small aerodynamic diameter and a high index of refraction.[4] Aerodynamic diameter is an indicator of how well a seed particle velocity matches that of the surrounding fluid. If the aerodynamic diameter is small, the particle velocity can be assumed to be equal to the velocity of the surrounding fluid. Traditional seed materials include smoke, olive oil, kerosene, and diethylhexylsebacate (DEHS). Polystyrene latex microsphere particles (PSLs) have also been used extensively as seed materials for PIV and LDV measurements due to their low aerodynamic diameter and high refractive index, which results in higher intensity Mie scattering when they are illuminated with laser light.[4] Although these properties enable the seed material to closely emulate the flow characteristics and be readily detected, measurements made close to a surface are difficult to perform due to the reflectivity of the surface itself. With fluorescent particles, near-surface imaging and PIV measurements are possible.[5] The fluorescent PIV technique uses an optical filter to block all surface reflections and only transmits the longer wavelength fluorescent light from seed particles. Similarly, wind tunnel researchers are interested in

Received: June 25, 2015
Accepted: August 31, 2015
Published: August 31, 2015

DOI: 10.1021/acsami.5b05584
ACS Appl. Mater. Interfaces 2015, 7, 20714−20725

being able to accurately measure the airflow velocity simultaneously with other airflow characteristics, i.e., temperature, concentration, etc. For example, noise in hot jets has a contribution from temperature fluctuations in a term due to turbulent enthalpy flux.[6] Therefore, if the thermal properties of an airflow can be accurately determined, modifications can be made to the hot jets to mitigate these fluctuations. Additionally, knowledge about local temperature in an airflow can give information about density or pressure through the ideal gas law.

PSLs are synthesized using either dispersion[7−9] or emulsion[10] polymerization. Additional methods related to emulsion polymerization include soap-free or surfactant-free emulsion polymerization. In aqueous emulsion polymerization, a water-insoluble monomer is polymerized using a radical initiator that introduces surface-active chemical species. Potassium persulfate, for which the decomposition kinetics are well-known,[11,12] is commonly used as the radical initiator, although more stable radicals, such as TEMPO,[13] have been investigated. This aqueous-phase polymerization process results in relatively low molecular weight polymeric species, 10^5 g/mol,[7] which coagulate until enough surface active groups are present to stabilize a colloidal dispersion through electrostatic interactions. Through this process, PSLs can be synthesized with particle diameters up to several microns with relatively narrow size distribution and without the need to introduce smaller seed particles. Although there remain many unanswered questions regarding the mechanism of particle growth in these polymerization reactions, recent results suggest that competition between particle nuclei for available monomer and radical species occurs until all the reactive species are consumed.[14] Microphase inversion of polystyrene oligomer nuclei (20−30 nm) into a water:acetone solution enabled observation of in situ particle diameter determination as the polystyrene nuclei were stabilized without the need for mechanical agitation. To observe the competitive kinetics of particle growth, 300 nm polystyrene seed particles were introduced early in the polymerization reaction. Within 48 h, two particle diameter modes, observed by dynamic light scattering (DLS), merged into a single mode slightly greater than 300 nm. By observing the growth rates of the polystyrene nuclei relative to the polystyrene seed particles, the authors were able to verify that the polystyrene nuclei were growing significantly faster in radius than the polystyrene seed particles.[14] This work suggests that once polystyrene oligomer nuclei are formed the particle size distribution should increase until a threshold radius is reached where the particles are stabilized, i.e., no further coagulation occurs. PSLs with diameters >3 μm were synthesized by extending the oligomer nucleation period through a dropwise monomer addition procedure conducted in methanol.[15] In this process, fewer oligomer nuclei were formed, relative to batchwise PSL synthesis, and subsequent monomer addition resulted in particle growth rather than additional nuclei generation.

In typical emulsion polymerization, the stable colloidal particle radius depends upon several parameters: monomer concentration, initiator concentration, the presence of a dispersion stabilizer, and reaction temperature, among other variables. Initiator concentration and the relative concentration of initiator to monomer have been reported to be primary factors dictating the ultimate PSL diameter, with an average surface area for each sulfate group being required to stabilize the PSLs.[16] Coagulation resulting in particle growth will occur when polystyrene nuclei with average surface area per sulfate groups exceed a critical value. Radical decomposition of potassium persulfate followed by polymerization initiation results in incorporation of sulfate groups within the particle nucleus, most likely present on the particle surface. Incorporation of greater amounts of initiator decreases the polystyrene oligomer length and increases the degree of sulfate functionalization resulting in smaller particles. As the surface area has a quadratic dependence on radius and volume has a cubic dependence on radius, increasing the initiator concentration will stabilize a greater surface area of generated PSLs, resulting in a lower average radius.

Equally important is the ionic strength of the aqueous solution. Increasing ionic strength, including ions generated from addition of the initiator, increases the particle diameter requisite to initiate coagulation. Goodwin et al. determined the range of ionic strengths amenable to formation of polystyrene PLSs in aqueous solutions to be from 10^{-7} to 10^{-5} M.[17] Variation of the electrolyte composition indicated further interactions depending on the charge of the cationic and anionic species.

For PSLs to be used as seed material in LIF experiments, the integration of highly fluorescent dyes in the PSLs at concentrations great enough to enable detection in the airflow is critical. Several techniques have been utilized to incorporate dye materials in particles and can basically be split into two approaches, incorporation of the dye during particle synthesis and incorporation after particle synthesis. Incorporation of dye onto existing particles can be achieved on just the surface through adsorption[18−20] or into the particle matrix by particle swelling followed by solvent exchange.[21,22] However, these methodologies do not yield particles with homogeneous distribution of dye within the particle matrix; i.e., there is likely a concentration gradient with the greatest concentration at the particle surface and the lowest concentration at the particle core. Similarly, since the dye addition is a secondary process, there may be inconsistent dye concentration between particles. Incorporation of the dye during the particle synthesis should enable even distribution of the dye throughout the particle matrix.[23] This is of significance since signal uniformity, along with narrow particle size distribution, will improve the accuracy of collected LIF data. This has been successfully demonstrated on much smaller particles generated through miniemulsion polymerization techniques.[24,25] In fact, Taniguchi et al. observed a more even dye distribution within particles that had a pyrene dye encapsulated within the particle polymer matrix when compared to a pyrene dye that was covalently bound in the polymer backbone.[26] We previously reported the incorporation of numerous species (mostly xanthene derivatives) into PSLs during particle synthesis.[27,28] Both dichlorofluorescein (DCF) and members of the rhodamine family were found to readily incorporate into the PSLs during the synthesis process. Despite having desirable experimental characteristics, some of these dyes have been classified as potentially toxic and carcinogenic by the International Agency for Research on Cancer.[29] Therefore, many dyes, rhodamines in particular, are not likely to be used for wind tunnel testing. Kiton Red 620 (KR620, Figure 1), however, is a potentially promising dye for use in a LIF seed material due to its nontoxicity (it is used as a dye for textiles and in some foods)[30,31] as well as its strong spectral properties and demonstrated temperature dependence.[27]

In this work, KR620-doped PSLs were synthesized via emulsifier-free emulsion polymerization. Initial experimentation

DOI: 10.1021/acsami.5b05584
ACS Appl. Mater. Interfaces 2015, 7, 20714−20725

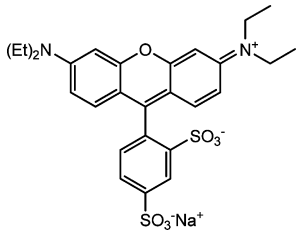

Figure 1. Structure of Kiton Red 620 (KR620).

with PSL synthesis indicated that the pH of the solution changed from approximately 7 to less than 3. This likely resulted in the formation of surface hydroxyl functionalities due to the hydrolysis of sulfate groups.[7] Therefore, inclusion of sodium bicarbonate was evaluated as an approach to maintain a stable pH throughout the polymerization reaction. Initial experimentation with incorporation of KR620 into PSLs was not successful, potentially due to the anionic charge present in the KR620 molecule. This could arise from electrostatic repulsion by sulfate, hydroxyl, or other anionic groups that populate the PSL surface. Similarly, rhodamine 6G, which is a cation, was determined to not readily adsorb on the surface of particles with surface cationic functionalities.[18] Likewise, the association of malachite green with particles was found to depend on the surface charge of the particle.[19] To reduce variability, both initiator concentration and stir speed were held constant; these experimental parameters have been demonstrated to impact PSL size and size distribution.[32] With all of these experimental variables, a design of experiments (DOE) was utilized to most efficiently explore the design space. The DOE method involves conducting a series of tests in which purposeful changes are made to input variables of a system. Then, the effects on output variables are measured. This method is designed to maximize the amount of information gained with a minimum number of experiments. This is done by varying factors simultaneously, instead of individually.[7]

2. EXPERIMENTAL SECTION

Design of Experiments Parameters. The above procedure involves many variables that could affect the results of the reaction. Therefore, design of experiments was utilized to investigate the effect of four factors: the mole ratio of styrenesulfonate, SS, to styrene (SS/S), and the amounts of KR620, polydiallyldimethylammonium chloride (polyD), and sodium bicarbonate buffer used in the reaction. The design used was a 4-factor, 2-level, response surface design with 8 center points (Table 1). For these experiments, the four factors were varied between a "high" level and a "low" level, + and− signs in Table 1. This gives a total of 16 combinations. Additionally, 8 center points were included, indicated as "M" in Table 1. Center points are tests for which each factor is held at the halfway point between the "high" and "low" levels. These center points were included to provide statistical power by estimating the repeatability of the experiments. They also provide a third point in addition to the "high" and "low" point, which allows one to move past a linear regression and estimate curvature.[33] In order to synthesize the necessary number of batches, two reactors were required. Therefore, the design included blocking the experiments for each reactor, which enabled elimination of unforeseen discrepancies in the results obtained from each reactor. Similarly, the order in which each experimental run was performed was randomized (see Experiment # vs Run # columns in Table 1) to remove any systemic errors in the data collected and enable thorough evaluation of the contributions from each factor. After completing each experiment, several output variables were measured. These included measurements of the particle size and distribution, the relative fluorescent signal, and the amount of leaching that occurred. PSL characterization results were utilized to generate a model for each response factor. All of the variables for a quadratic fit were initially considered, with only those generating significant p values, values used to ascertain the statistical significance of each model term, retained in the model.

Table 1. Design of Experiments' Synthetic Outline for Each Factor

experiment #	run #	block	KR620	SS/S ratio	PolyD	$NaHCO_3$
PSL-1	14	2	-	-	-	-
PSL-2	1	1	+	-	-	-
PSL-3	8	1	-	+	-	-
PSL-4	23	2	+	+	-	-
PSL-5	5	1	-	-	+	-
PSL-6	20	2	+	-	+	-
PSL-7	21	2	-	+	+	-
PSL-8	4	1	+	+	+	-
PSL-9	10	1	-	-	-	+
PSL-10	18	2	+	-	-	+
PSL-11	17	2	-	+	-	+
PSL-12	12	1	+	+	-	+
PSL-13	22	2	-	-	+	+
PSL-14	2	1	+	-	+	+
PSL-15	7	1	-	+	+	+
PSL-16	16	2	+	+	+	+
PSL-17	9	1	M	M	M	M
PSL-18	3	1	M	M	M	M
PSL-19	6	1	M	M	M	M
PSL-20	11	1	M	M	M	M
PSL-21	13	2	M	M	M	M
PSL-22	24	2	M	M	M	M
PSL-23	15	2	M	M	M	M
PSL-24	19	2	M	M	M	M

The range for the low and high levels for each factor needed to be determined prior to starting the experiments. On the basis of previous experience,[27] conservative ranges that would still result in changes to the experimental outcome were identified (Table 2). For midpoint experiments, the values for each factor are simply the middle of the experimental range. All of the quantities were calculated for a target solution volume of 250 mL. The responses identified, where a response is the result from characterization of the PSLs, along with the target for each response are indicated in Table 3. The goal for particle size was selected based on a typical particle size for use in airflow seeding, while the goal for particle size distribution was based

Table 2. Range for Each Factor Evaluated in the DOE Experimental Outline

factor	low level	mid level	high level
Kiton red 620, mg	5	27.5	50
SS/S molar ratio	0	0.03	0.06
PolyD, g	0	0.5	1.0
$NaHCO_3$, g	0	0.75	1.5

DOI: 10.1021/acsami.5b05584
ACS Appl. Mater. Interfaces 2015, 7, 20714−20725

Table 3. DOE Response Parameters and Goals

response	goal
mean particle diameter	1 μm
particle size distribution (i.e., magnitude of standard deviation (σ))	minimize σ ($\leq$25%)
fluorescent emission	maximize
dye retention (ret%)	maximize
leach solution absorbance at 400 nm	minimize

on an attempt to minimize the propagation of error in particle size to error in measured airflow properties. Maximizing the fluorescent emission would enable the greatest signal-to-noise ratio. The dye retention response is the percentage of KR620 retained within the PSLs after leaching experiments. Measuring the Rayleigh scattering of the filtrate solution from leaching experiments at 400 nm provides insight into the portion of soluble polymeric material, which is undesirable, generated during the PSL synthesis.

Materials and Instrumentation. Styrene (Sigma-Aldrich) was distilled prior to use to remove the inhibitor, 4-*tert*-butylcatechol. The remaining reagents were used as received. Particle size measurements were conducted on a Particle Sizing System model 780 AccuSizer.

Polystyrene Microsphere Synthesis and Characterization—Small Scale. The synthesis of PSLs was done in a batchwise process, with batch volumes of approximately 250 mL (see Table S1 in Supporting Information for the actual quantities used in each experimental run). A 500 mL reaction kettle was fitted with a mechanical stir rod, a water-cooled condensation column, and a nitrogen inlet. The reaction kettle lid was secured and sealed to the kettle by using a small amount of vacuum grease and a fitted clamp. The kettle was placed in an oil bath that also contained a thermocouple to track and control its temperature. As previously mentioned, two reaction setups located adjacent to one another to minimize environmental factor impact were utilized to complete all of the synthetic trials outlined in the DOE matrix.

Although each synthetic trial was slightly different depending on what parameters were being evaluated, a general description is provided. Sodium bicarbonate (the amount depending upon the synthetic trial) was added to a beaker containing deionized water (250 mL, 18 MΩ). A portion of the buffer/water solution (approximately 50 mL) was placed in a beaker and sparged with nitrogen (N_2) at a high flow rate for approximately 30 min to remove any dissolved oxygen in the solution, at which point 8 mL of the sparged buffer solution was placed in a small beaker, covered, and placed in an oven at 70 °C. Concurrent to this, a portion of the buffer solution (approximately 50 mL) was added to the reaction kettle. KR620 (the amount depending upon the synthetic trial) was mixed into 100 mL of the buffer solution and added to the reaction kettle. PolyD (the amount depending upon the synthetic trial) was rinsed into the reaction kettle with 50 mL of the buffer solution. Styrene (freshly distilled) and styrenesulfonate (the quantity of both components depended upon the synthetic trial) were then added to the reaction kettle. The remaining sparged buffer solution was used to rinse any residues into the kettle. The mixture in the kettle was sparged with N_2 and stirred at 60 rpm for approximately 60 min. Once the sparging was complete, the N_2 gas flow rate was reduced, the sparging tube replaced with a N_2 source to maintain an inert atmosphere, and the stir rate increased to 250 rpm. The temperature of the hot plate was then set to 90 °C; based on previous empirical results, an oil bath temperature of approximately 90 °C resulted in a reaction solution temperature of 70 °C. After thermal equilibration, approximately 0.2 g of $K_2S_2O_8$ was added to the 8 mL of heated, sparged solution and subsequently added to the reaction kettle. The mixture was stirred at 250 rpm at constant temperature under an inert atmosphere for approximately 21 h. This duration was selected based on the literature[14] and previous experience indicating that the particle size distribution continues to decrease over at least a 19 h period, if not longer. Next, the kettle was allowed to cool to ambient temperature, and the solution was poured through a funnel using cheese cloth to capture any large agglomerates of polystyrene material.

As can be seen in Table 1, the composition of the midpoint experiments (PSL batches PSL-17 to PSL-24) was identical. This was performed to both ascertain curvature for relationships between the low level and high level conditions for each factor and to evaluate reproducibility. In addition to this, several of the PSL batches were ran in duplicate, with some compositions, especially those that did not yield PSLs upon the first attempt, being ran in triplicate.

Polystyrene Microsphere Synthesis and Characterization—Large Scale. The ultimate goal of this work was to identify reaction conditions most likely to yield highly fluorescent particles that were approximately 1 μm in diameter and exhibited minimal leaching of the dye into the suspension solution, water (Table 2). These conditions, once determined by the design of experiments statistical analysis, were utilized to scale up and synthesize an 8× larger batch (approximately 2 L at 9 wt % solids) of KR620-doped PSLs for use in air flow seeding experiments, described below. The synthetic procedure for generation of PSLs of controlled diameter on this scale has been previously reported[34] but was modified for this work. Briefly, a large reaction kettle, fitted inside a heating mantle, was outfitted with a thermocouple, mechanical stir paddle, a water-cooled condenser, and a sparging tube. The kettle was charged with approximately 2 L of deionized water (250 mL, 18 MΩ), freshly distilled styrene (187 g), sodium bicarbonate (12 g), polyD (0.8 g), KR620 (0.4 g), and styrenesulfonate (20 g). This solution was heated to 70 °C and sparged with N_2 (400 sccm) for 45 min while being stirred at 150 rpm. Approximately 30 mL of deionized water was placed in a beaker which was heated to approximately 70 °C. After sparging, the sparging tube was replaced with a coldfinger, and the N_2 flow was diverted through the thermocouple adapter at the same flow rate to maintain an inert atmosphere over the reaction solution. The stir rate was increased to 250 rpm, and 1.6 g of $K_2S_2O_8$ was added to 30 mL of heated water and subsequently added to the reaction kettle. The reaction was stirred for 21 h, cooled to ambient temperature, and poured through cheesecloth to remove large agglomerated polystyrene materials.

Spectroscopic Characterization of PSLs. Fluorescent emission of each batch of PSLs was collected by preparing a microscope slide through soaking in 2 N NaOH for approximately 10 min followed by applying a layer of particle solution to the slide and drying in an oven. The slide was placed below a low power, continuous wave Nd:YAG laser that passed through a concave lens to broaden the beam. Fluorescent emission was collected by a fiber optic after passing through a Semrock 532 nm notch filter. The fiber optic transferred the signal to an Ocean Optics HR2000 spectrometer, and the data were analyzed using SpectraSuite software. The collected spectra were processed by subtracting

DOI: 10.1021/acsami.5b05584
ACS Appl. Mater. Interfaces 2015, 7, 20714−20725

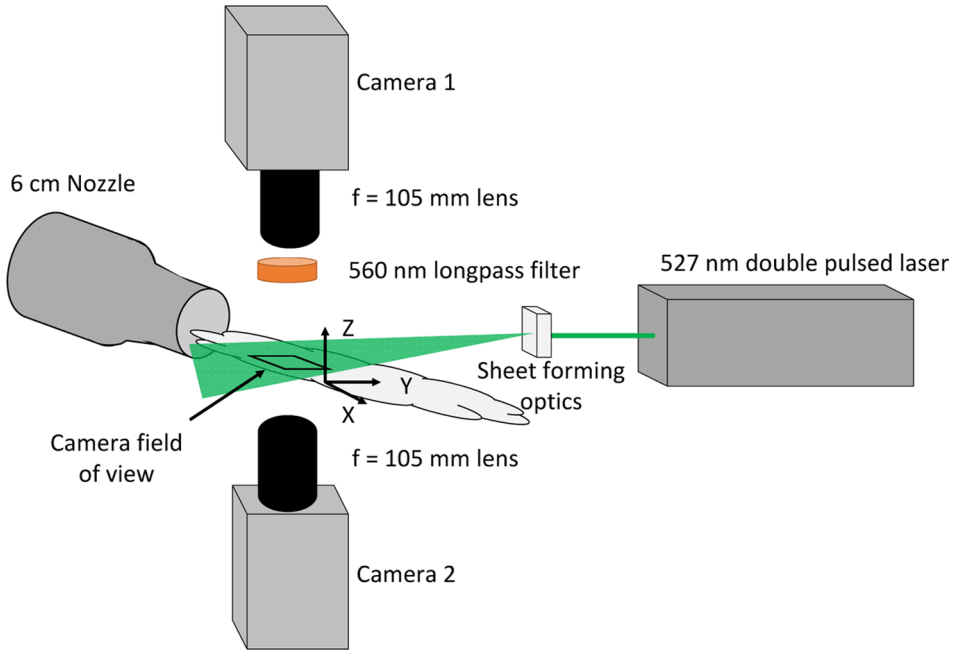

Figure 2. Experimental PIV test setup.

the background intensity and correcting for the relative spectral response of the detection system.[35]

Several additional factors were involved in order to enable accurate comparison of the spectral data. The thickness of the sample plays a large role in signal strength. Therefore, approximately 0.2 mL of the PSL suspension was used for sample generation. The solution was manually spread using a glass pipet over approximately the same surface area of the prepared slide to minimize local variation in concentration. Still, the location of excitation on the sample can affect the measured signal strength with fluorescent intensity varying as much as 50% for different surface regions. Great care was taken to ascertain an average fluorescent emission intensity on the PSL-covered surface; however, the relative fluorescent emission intensity should be considered a largely qualitative measurement. The measurements were collected in this manner to best represent the particle state when present in a wind tunnel environment, where the solvent is understood to rapidly evaporate due to expansion resulting in dry particles.

Microscopic Characterization of PSLs. To prepare samples for optical characterization, approximately 15 mL of the PSL solution was centrifuged (Thermo Scientific Sorvall ST8) at 3000 rpm for 5−10 min. The supernatant was poured off, and the PSLs were dispersed in deionized water (18 MΩ) followed by sonication for approximately 2 min. Approximately 0.2 mL of the solution was deposited onto glass slides that had been cleaned in a 2 N NaOH aqueous solution for 10 min. The solution was spread over the glass slide surface and allowed to evaporate. Optical micrographs were collected using an AXIO Imager.Z1M (Zeiss) equipped with an AxioCam MRc5 camera. Confocal fluorescence micrographs were collected on the same instrument outfitted with an LSM 5 Exciter that provided excitation at 543 nm. A 560 nm long pass filter was utilized to only collect fluorescent emission. The optical gain necessary to attenuate the intensity of each image to a common value was recorded in order to enable comparison of the relative intensity of the collected fluorescent images.

Kiton Red Leaching Studies. A leaching study was conducted to determine if KR620 was successfully incorporated into the PSLs or simply dissolved in the solution. To assess this, a PSL suspension (10 mL) was placed in a centrifuge tube and spun at 4500 rpm for 45 min (Centra CL3). The absorption spectrum of the centrifugate was collected on a PerkinElmer Lambda 900 UV spectrometer. Two factors were determined from the collected spectrum, the dye concentration and the degree of light scattering. To determine the dye concentration, a Beer−Lambert plot of KR620 absorbance values (λ_{max} = 564 nm) at known concentrations was generated to determine the molar extinction coefficient ε = 110 mM^{-1} cm^{-1} (an ε of 118 mM^{-1} cm^{-1} in ethanol was reported from Exciton).[36] This was used to determine the KR620 concentration in the centrifugate. The collected spectra were corrected for Rayleigh scattering to determine the absorbance at λ_{max} arising solely from KR620. Calculated concentrations were then compared to the KR620 concentration in the PSL batch to determine a % dye retention value (ret%) according to

$$\text{ret\%} = 100^{*}\frac{[\text{KR620}]_0 - [\text{KR620}]_{\text{CF}}}{[\text{KR620}]_0} \quad (1)$$

where $[\text{KR620}]_0$ and $[\text{KR620}]_{\text{CF}}$ are the KR620 concentrations calculated for the PSL batch and the centrifugate, respectively. For this work, a lower concentration of KR620 in the centrifugate did not necessarily indicate greater retention of the dye in the PSL. This arose from the possibility of KR620 being retained in agglomerated polystyrene material from the reaction kettle. In that case, the ret% value would be high, indicating that the solution concentration of KR620 was low. Therefore, both ret% and fluorescent emission intensity values were considered to ascertain the actual KR620 loading of the PSLs.

The generation of water-soluble colloidal material was not desired, and the amount of Rayleigh scattering by the centrifugate was assumed to be related to the production of these unwanted materials. The absorbance at 400 nm of spectra not corrected for scattering was used to compare the extent of

DOI: 10.1021/acsami.5b05584
ACS Appl. Mater. Interfaces 2015, 7, 20714−20725

water-soluble colloidal material synthesis in each batch. At this wavelength, the Rayleigh scattering due to water is neglible for the 1 cm path length quartz cuvettes used in this work.

KR620 PIV and Signal Characterization Experiments. The PIV data included in this paper were recorded from the experimental setup seen in Figure 2. Tests used either one or two Photron SA1.1 Fastcam high-speed cameras with a 1024 × 1024 pixel resolution and 12-bit intensity digitization. The cameras were positioned above and below the airflow and perpendicular to the laser sheet for 2D PIV. Two Sigma 105 mm f/2.8 EX DG macrolenses were used with the cameras to obtain a close-up image of the flow. The camera fields of view for all experiments were approximately 30 × 30 mm^2.

For fluorescence imaging, a 560 nm long pass filter (Omega Optical, 560 HLP) was attached to the lens, blocking out all Mie-scattered light from the particles and only allowing particle-emitted fluorescent light to be captured by the camera. A 527 nm dual-head Nd:YLF laser (Photonics model DM30) was used at approximately 23 mJ/pulse to illuminate the flow and was controlled simultaneously with the camera by LaVision's DaVis software (package V), recording at 2.5 kHz for time-resolved images. Finally, an $f = -20$ mm cylindrical lens was used to form a thin laser sheet at the nozzle exit in the orientation depicted in Figure 2. The laser sheet measured approximately 1.25 mm thick and 3.5 cm wide in the measurement plane at the nozzle exit. The cameras imaged a region of flow about 8 cm from the nozzle exit.

The KR620-doped PSL particles were seeded using two Air-o-Swiss 7146 ultrasonic humidifiers. Seed was introduced well upstream of the nozzle exit into the blower inlet, where it mixed with the air at room temperature and flowed through a nozzle of 6 cm exit diameter. The airflow at the exit for the PIV tests in this paper was about 33 m/s, corresponding to a Reynolds number per meter of approximately 2 000 000 m^{-1}. Before each test, the KR620 particle solution was mixed in equal proportions with distilled water and was sonicated for 15 min in an L&R Quantrex 90H ultrasonic disruptor to prevent particle agglomeration. The mixture was then removed from the disruptor and placed immediately into the vaporizer. The two-camera setup seen in Figure 2 was used to image Mie-scattered and fluorescent light simultaneously. Camera 2 was placed on a 3-axis traverse and 3-axis camera mount so that it could be maneuvered to image the same particles in the flow.

In these tests, the near-surface flow over a blunt leading edge flat aluminum plate was measured. As seen in Figure 3A, the plate was oriented parallel to the flow exiting the nozzle and perpendicular to the incident laser sheet. The dimensions of the flat plate are shown in Figure 3B. For these tests, a set of 2000 double-frame fluorescent images were obtained with the filter over the lens of camera 1, and another 2000 double-frame images were simultaneously recorded by Camera 2 of the Mie-scattered signal. Then, the filter was quickly removed, and another 2000 double-frame images were recorded of the Mie-scattered signal.

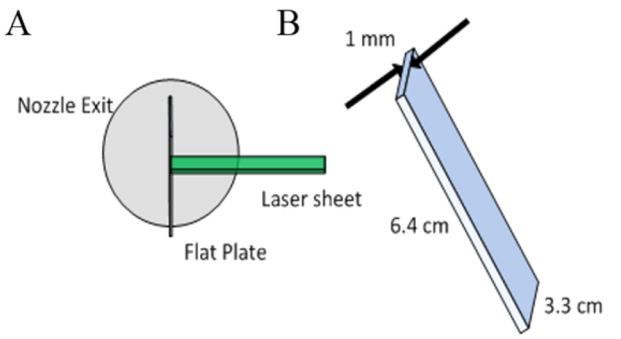

Figure 3. (a) Parallel flat plate orientation and (b) plate dimensions. Flow is out of the page.

3. RESULTS AND DISCUSSION

PSL Synthesis and Characterization. PSLs were generated as aqueous suspensions at approximately 9 wt % solids. Although only three different KR620 concentrations were utilized throughout this work, the resultant particle solution appearances varied considerably. The solution color varied from white, indicating no retention of KR620, to deep purple and various shades in between. After the PSLs were synthesized, large agglomerated polystyrene particles were observed that were strongly adhered to the stir paddle on several occasions indicating that the styrene had not been fully dispersed in the solution. In a few instances that the solution was very light in color, the polystyrene agglomerate was deeply colored, indicating that the dye had preferentially segregated into the amorphous polystyrene. The solution opacity changed from empirically transparent, indicating no particle formation, to cloudy, indicating either particle synthesis or emulsion formation. For compositions that provided relatively large particles, i.e., particle diameter >0.65 μm, after 24 h, particle formation would be apparent from settling of PSLs in the bottom of the sample bottle. An emulsion, with soluble polymeric materials, would not undergo this gravitational settling. As an example, Figure 4 displays the particle size

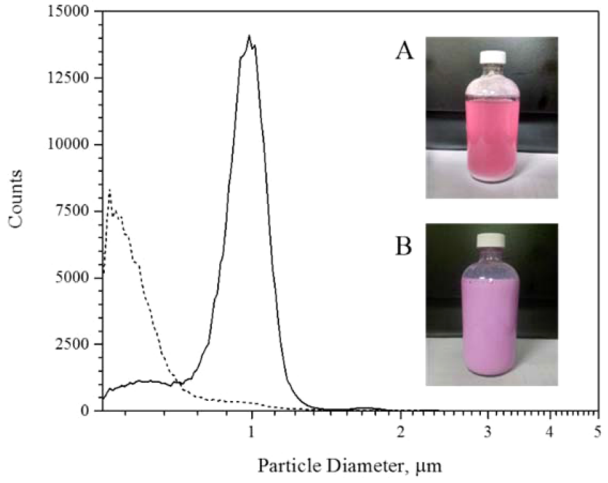

Figure 4. Particle size histograms for PSL-1 (solid line) and PSL-18 (dashed line). The insets are photographs of the PSL-1 (A) and PSL-18 (B) solutions after sitting undisturbed for several weeks.

histograms from two PSL batches generated in this work, PSL-1 and PSL-18. As can be seen from the inset images, the larger particles have settled to the bottom of the bottle in Figure 4A, while the smaller particles remained suspended in Figure 4B.

Several spectral properties of the PSLs were determined: fluorescent emission intensity of dried PSL samples as well as absorbance from KR620 and Rayleigh scattering at 400 nm from leach experiment solutions. The fluorescent emission was determined in the dried state (Figure 5A) to best reflect the state in which these PSLs would be used for airflow seeding in

DOI: 10.1021/acsami.5b05584
ACS Appl. Mater. Interfaces 2015, 7, 20714−20725

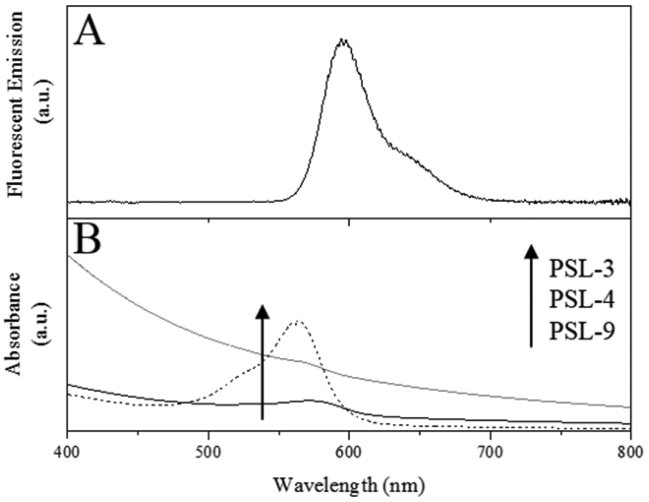

Figure 5. (A) Fluorescence emission spectrum of dried PSLs from PSL-8. (B) Absorbance spectra of centrifugate from leaching experiments on PSL-9 (black solid line), PSL-4 (black dashed line), and PSL-3 (gray solid line) displaying high dye retention, low dye retention, and a large concentration of water-soluble polymeric materials, respectively.

wind tunnel experiments. From leaching experiments, the dye retention (ret%) was determined by measuring the absorbance arising from KR620 in the centrifugate (Figure 5B) and using an experimentally determined molar extinction coefficient (ε = 110 mM^{-1} cm^{-1}) to calculate dye concentration. Rayleigh scattering arising from soluble polymeric material was also determined in this solution by observing the absorbance at 400 nm, a wavelength where no absorbance arises from either KR620 or polystyrene. Combined, all of these characterization experiments were utilized as responses for DOE analysis (Table 4).

Single Factor Influence—Kiton Red Concentration. On the basis of preliminary experiments, attempts to incorporate KR620 into PSLs comprised solely of polystyrene did not yield viable fluorescent PSLs. Nevertheless, the impact that inclusion of KR620 over the concentration range studied in this work has on the polymerization and particle synthesis was critical to understanding how incorporation of other components changed the PSL dispersion properties. As can be seen from Table 4, PSL batches PSL-1 and PSL-2, consisting of the low and high KR620 concentration factor limits, respectively, exhibited significantly different properties. For PSL-1, approximately 1 μm particles were generated, and although the determined dye retention is high, the fluorescent emission is relatively low. The relative scattering at 400 nm, a qualitative measure of the amount of solubilized, micellar oligomeric materials, was low. PSL-2, generated with the high KR620 concentration, had a much lower particle size, 0.58 μm, and a much greater relative scattering value at 400 nm. Both of these results indicated that the presence of KR620 was disrupting the polymerization process, potentially due to the charged nature of the dye. Although the leaching study indicated that the dye was retained (87% retention), the relative fluorescent emission was very low. This indicated that the KR620 was not initially captured by the PSLs during synthesis and likely was retained in the agglomerated polystyrene material adhered to the stir paddle. Thus, without additional components to retain the KR620 while not further disrupting the polymerization, the pure polystyrene microspheres were determined to be unable to retain KR620 in a sufficient quantity to yield highly fluorescent particles while maintaining stable particle synthesis conditions. Although there are other single factor influences that could be considered regarding their influence on the polymerization, they were not evaluated in this work as they would not yield fluorescent particles.

Table 4. PSL Characterization Results

experiment #	mean particle diameter (μm)	relative fluorescent emission (au)	ret%	relative scattering at 400 nm (au)
PSL-1	0.97 ± 0.13	0.01	97%	0.05
PSL-2	0.58 ± 0.10	0.02	88%	0.20
PSL-3	0.59 ± 0.09	0.07	23%	0.80
PSL-4	0.60 ± 0.18	0.43	13%	0.17
PSL-5	0.74 ± 0.37	0.01	100%	0.26
PSL-6	0.66 ± 0.54	0.01	92%	0.45
PSL-7	--	--	--	--
PSL-8	1.36 ± 0.60	0.52	54%	0.16
PSL-9	0.71 ± 0.20	0.10	84%	0.21
PSL-10	0.65 ± 0.30	0.02	57%	0.28
PSL-11	0.77 ± 0.99	0.89	26%	0.71
PSL-12	0.58 ± 0.19	0.63	15%	0.54
PSL-13	0.70 ± 0.29	0.00	100%	0.30
PSL-14	1.59 ± 1.14	0.11	89%	0.30
PSL-15	0.90 ± 0.83	0.33	22%	0.44
PSL-16	--	--	--	--
PSL-17	0.62 ± 0.19	0.34	−16%	0.59
PSL-18	0.63 ± 0.31	1.00	20%	0.76
PSL-19	0.60 ± 0.10	0.90	−26%	0.52
PSL-20	0.59 ± 0.10	0.40	20%	0.51
PSL-21	0.77 ± 0.27	0.74	−31%	0.53
PSL-22	0.61 ± 0.26	0.34	48%	0.72
PSL-23	0.59 ± 0.13	0.85	46%	0.47
PSL-24	0.64 ± 0.11	0.78	37%	1.00

Before discussing multiple factor influences, it is important to discuss how well the response factors accurately measure the intended PSL properties. Of particular importance is the correlation between fluorescent emission intensity and ret%. This is of interest since, for some compositions, there are three places KR620 could be most strongly associated: with the PSLs, the aqueous phase, or the large insoluble polystyrene agglomerate. Likewise, collection and comparison of solid-state fluorescent emission properties is extremely difficult, and as was mentioned in the Experimental Section, great care was taken to collect fluorescent emission values representative of the prepared samples. When plotted against each other, these two response factors exhibited an inverse relationship with some of the highest ret% values arising from PSL compositions with the lowest relative fluorescent emission values (data not shown). This indicated that, for these compositions, a majority of the dye was retained within the PSL agglomerate. This was an important result and was considered when analyzing dual and multifactor influences as described below.

Dual Factor Influences. Comparison of two factor influences was relatively straightforward since the combinations of greatest relevance had KR620 concentration as one of the factors. Addition of styrenesulfonate, at low KR620 concentrations, PSL-3, resulted in a significant reduction in particle size and an increase in relative scattering at 400 nm. Similarly, the dye retention dropped precipitously. All of these results indicated that the addition of styrenesulfonate increased the

DOI: 10.1021/acsami.5b05584
ACS Appl. Mater. Interfaces 2015, 7, 20714−20725

solubility of the polymeric materials. Interestingly, the relative fluorescent emission increased slightly. One possibility is that the presence of the styrenesulfonate enabled better dispersion of the KR620 in the polymeric matrix once dried. At high KR620 and styrenesulfonate concentrations, PSL-4, the particle size is approximately the same as PSL-2, batch with the same KR620 concentration and no styrenesulfonate. Although the relative fluorescent emission increased by a factor of 36, the retention was very low.

PolyD was incorporated in the dispersion for the purpose of electrostatically trapping KR620 molecules within the PSLs. Since PSLs synthesized via dispersion polymerization using potassium persulfate decomposition as a radical source are known to have surfaces populated by sulfate groups, the polyD should preferentially interact at the particle surface. This interaction was envisioned to generate an electrostatic double layer at the PSL surface that would prevent KR620 molecules from diffusing out of the PSLs once generated. To determine whether this approach was successful or not, batches PSL-1 and PSL-5 can be compared. As can be seen in Table 4, although the particle size is reduced slightly and the standard deviation increased along with the relative scattering at 400 nm, the dye retention was maintained if not improved slightly. The relative fluorescent emission was low, which would be expected at this KR620 concentration. The decreased particle size and increased standard deviation and scattering values could arise from the polyD acting to solubilize small oligomeric species similar to what was observed with incorporation of styrenesulfonate. At high KR620 and polyD concentrations, PSL-6, the particle size increased slightly as did the relative scattering at 400 nm. Although the determined ret% increased slightly, relative to PSL-2, the relative fluorescent emission actually decreased. Therefore, the addition of polyD was not enough to prevent destabilization of the dispersion polymerization arising from increased KR620 concentration.

Although it has been reported that KR620 emission is relatively insensitive to pH,[37] preliminary results indicated that the fluorescent properties of KR620-doped PSLs were influenced by pH with a slightly basic pH yielding higher fluorescent emission intensity. As the pH of the PSL solution without any additional components, i.e., a dispersion generated from styrene monomer and potassium persulfate alone, was determined to be slightly acidic, a slightly basic buffer system, sodium bicarbonate, was utilized in this work. When the buffer was included at low KR620 concentrations, PSL-9, the relative scattering at 400 nm increased, relative to PSL-1, suggesting an increase in soluble polymeric material. Although the ret% decreased (84%) relative to PSL-1, the relative fluorescent emission increased 8 times, which is significant considering the fact that the dye concentration did not change. With the inclusion of the buffer at the high KR620 concentration range, PSL-10, there was a slight decrease in particle size, relative to PSL-9, as well as a decrease in fluorescent emission intensity, which is surprising considering that PSL-10 was generated with an order of magnitude greater KR620 than PSL-9. The ret% also decreased, relative to PSL-9, suggesting again that the PSLs cannot retain all of the dye at this KR620 loading level.

Multifactor Influences. On the basis of all of the dual-factor influenced properties identified here, there are several combinations of materials that could be anticipated to provide both promising PSLs and poor performing PSLs with respect to target particle size, dye retention, etc. For example, it could be anticipated that PSLs generated with both polyD and buffer should have moderate fluorescent emission properties, relatively high % retention values, and potentially low scattered light values. This combination was included in the DOE test matrix and corresponds to batches PSL-13 and PSL-14 for low and high KR620 concentrations, respectively. Surprisingly, PSL-13 did not exhibit improved properties relative to PSL-1 (batch comprised of only styrene and KR620), PSL-5 (batch comprised of styrene, KR620, and polyD), or PSL-9 (batch comprised of styrene, KR620, and buffer). PSL-14, however, exhibited properties that were superior, in most cases, to PSLs generated at this KR620 concentration without any other constituent, with just polyD, or with just the buffer: PSL-2, PSL-6, and PSL-10, respectively. Although the relative fluorescent emission was not great, it was higher than that determined for the other batches just mentioned, even though the KR620 concentration was equivalent in all cases. The results for PSL-14 suggested that the KR620 had a stronger affinity to associate with the PSLs, relative to the amorphous polymeric material. The % retention for PSL-14 was also comparable to these other batches.

As the intent of inclusion of both SS and polyD was to generate an electrostatic double layer that would act as a barrier to KR620 diffusion out of the PSLs, comparison of these batches was of interest. PSL-7 and PSL-8 are the combinations of these constituents at low and high KR620 concentrations, respectively. Inexplicably, no particles were synthesized under the conditions in PSL-7. The synthesis was repeated three times with no formation of particles. PSL-8, however, did result in particle fabrication with diameters >1 μm. Additionally, the fluorescent emission was greatest for PSL-8, relative to PSL-2 (batch consisting of only styrene and KR620), PSL-4 (batch consisting of styrene, SS, and KR620), and PSL-6 (batch consisting of styrene, polyD, and KR620). Although the % retention is somewhat lower in PSL-8, relative to PSL-2 or PSL-6, the very low fluorescent emission intensities measured for these two batches suggest that a majority of the dye had diffused into the amorphous polystyrene material retained in the reaction kettle. The relative scattering at 400 nm was also low for PSL-8, which suggested that a less significant portion of water-soluble material was generated under these reaction conditions.

Conversely, it could be envisioned that, based on the results from dual interactions described above, the combination of SS and buffer should result in very poor performing PSLs. These combinations are represented by PSL-11 and PSL-12 for low and high KR620 concentrations, respectively. Although both batches exhibited high fluorescent emission values, both also exhibited very low % retention values. Scattering at 400 nm was high in both cases indicating a significant formation of soluble polymeric material. Similar to what has been discussed before, the mean particle diameter was smaller for PSL-12, relative to PSL-11, again suggesting that, without introduction of components to preferentially interact with the KR620, the dye disrupts the polymerization reaction resulting in smaller particles.

Several of the PSL batch formulations were repeated including the midpoint formulations as well as other batches to ascertain variability in the resultant PSL properties. As can be seen in Table 4, even though the experimental parameters were nearly identical, the results from the midpoint experiments were variable. This is an important result and indicated that, upon transition to the large batch synthesis, some variability between predicted results and actual results should be expected.

DOI: 10.1021/acsami.5b05584
ACS Appl. Mater. Interfaces 2015, 7, 20714−20725

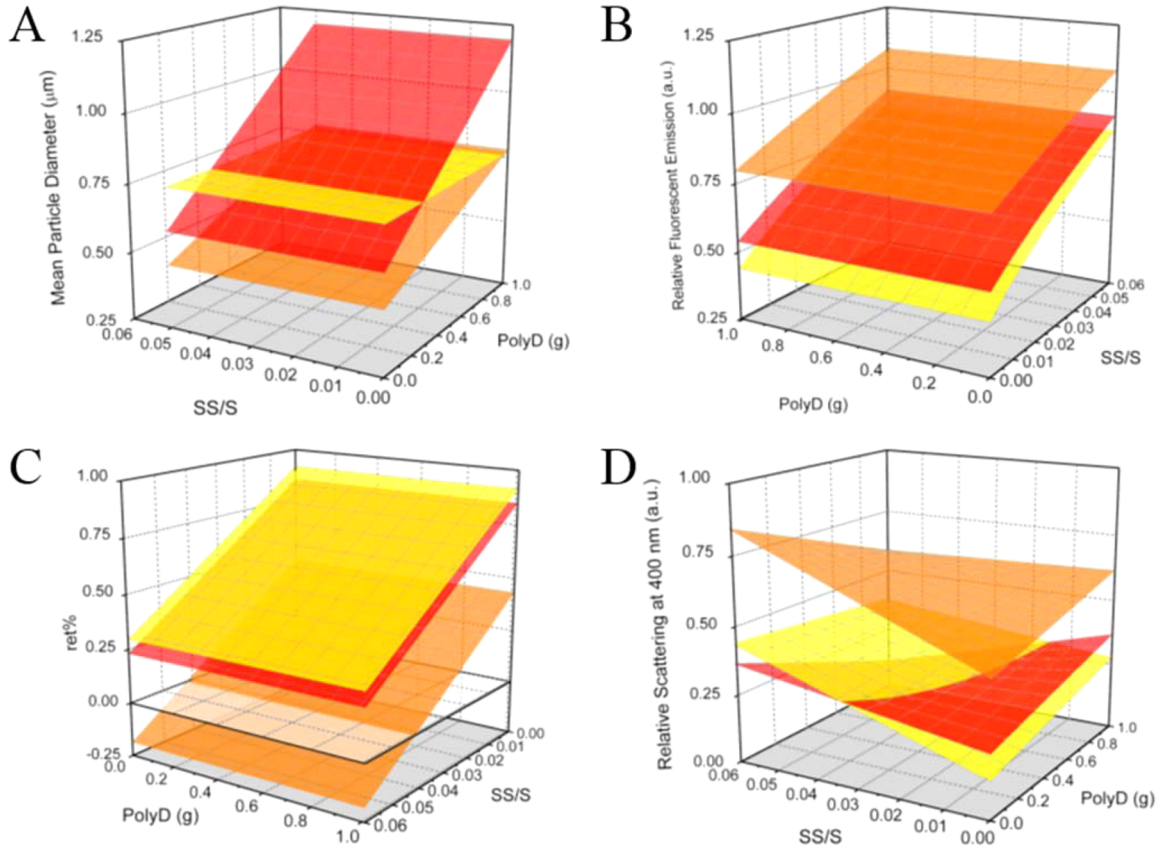

Figure 6. Surface plots of the empirical models for (A) mean particle diameter, (B) relative fluorescent emission, (C) retention %, and (D) relative scattering at 400 nm. These responses were plotted against PolyD mass and SS/S ratio at low, midrange, and high concentrations of KR620 and are indicated on the plots as yellow, orange, and red surfaces, respectively. The $NaHCO_3$ concentration was maximized in every case.

Likewise, this variability was anticipated to result in greater uncertainty in the DOE modeling of the response factors (see below). Although the particle size for these experiments was relatively consistent with an average value of 0.63 ± 0.09 μm, the normalized emission, ret% value, and normalized absorbance at 400 nm all varied considerably. The ret% values were low in all cases, and the normalized absorbance at 400 nm was high indicating that this composition was not amenable to generation of reliable PSLs capable of incorporating KR620 successfully. Similarly, the composition for PSL-6 was repeated with the PSL diameter determined to be 0.66 ± 0.54 μm and 0.74 ± 0.15 μm for the first and second batches, respectively. The other PSL parameters for these two batches exhibited similar agreement. As was previously mentioned, the compositions for PSL-7 and PSL-16 were generated in triplicate as the first attempt did not yield PSLs. These two compositions did not yield PSLs in any of the three attempts, and it was determined that these conditions were simply not amenable to particle generation.

To examine these multifactor influences further, statistical analysis was performed on the collected response parameter values using the input parameters and response factors described in Tables 2 and 3, respectively. PSL-7 and PSL-16 conditions were ignored in this analysis as they did not yield PSLs that could be characterized. By correlating each input with a response, the relative influence the input parameter conditions had on each response factor was determined. Model surfaces were generated indicating the expected value for each response calculated from relevant input parameter conditions (Figure 6). All of these plots were calculated at the upper $NaHCO_3$ concentration limit and the indicated KR620 concentration. The standard deviation and correlation coefficients of the resultant models for each response factor are reported in Table 5. Interestingly, $NaHCO_3$ was determined to impact only the relative fluorescent emission (Figure 6B). The mean particle diameter was determined to have no dependence on the presence of styrenesulfonate (Figure 6A). This response model had the lowest correlation coefficient (R^2 = 0.58), which, based on further review of the associated p-values for all of the model parameters, indicated that there were likely a myriad of weak relationships between the input parameters and the mean particle diameter. The model for ret% did not have any relevant terms associating with the presence of PolyD. This result may be somewhat ambiguous since, as mentioned previously, the ret % values must be considered along with the relative fluorescent emission values to ascertain the amount of KR620 retained in the particles. The inverse nature of the relationship between these two factors was reproduced in their corresponding

Table 5. DOE Model Fit Statistics

response factor	standard deviation	correlation coefficient (R^2)
mean particle diameter (μm)	0.19	0.58
standard deviation, σ (μm)	0.15	0.68
relative fluorescent emission (au)	0.16	0.82
ret%	0.24	0.73
relative scattering at 400 nm (au)	0.15	0.73

DOI: 10.1021/acsami.5b05584
ACS Appl. Mater. Interfaces 2015, 7, 20714−20725

models with the midrange KR620 concentration plots calculated to be the greatest relative fluorescent emission and lowest ret% surfaces. The standard deviation for the ret% model was large (0.24), likely due to the KR620 retained within the agglomerated polystyrene not being considered in the calculation of this response factor. The "relative scattering at 400 nm" response factor was determined to have the greatest number of input parameter dependencies (Figure 6D). This correlated well with the empirical relationships discussed previously indicating that each of the input parameters influence the stability of the synthesis emulsion and the solubility of small styrene oligomers.

Optical Characterization. Samples of PSLs dispersed on microscope slides were prepared, and optical and fluorescent emission micrographs were collected on them (Figure 7). As can be seen in Figure 7A, the PSLs generated from the PSL-1 formulation were relatively uniform in size. This correlated well with the low particle diameter standard deviation (13%) measured for this composition and resulted in more favorable monolayer formation relative to PSL-6 and PSL-9 samples with standard deviation values of 81% and 28%, respectively. The confocal fluorescent images of these samples, however, clearly show the spherical nature of all of the imaged batches and also demonstrate the relative uniformity of the emission intensity from individual particles. Although the relative emission intensities for PSL-1 and PSL-6 were measured to be low, 0.01 in both cases, the fluorescent emission was readily resolved on the confocal microscope. In an effort to compare the relative emission intensities collected on the confocal microscope, the optical gain was noted for each image collected. The optical gain was the lowest for PSL-24; i.e., the fluorescent emission intensity was the greatest, which was in agreement with the relative emission intensity values determined using the Nd:YAG laser excitation described previously.

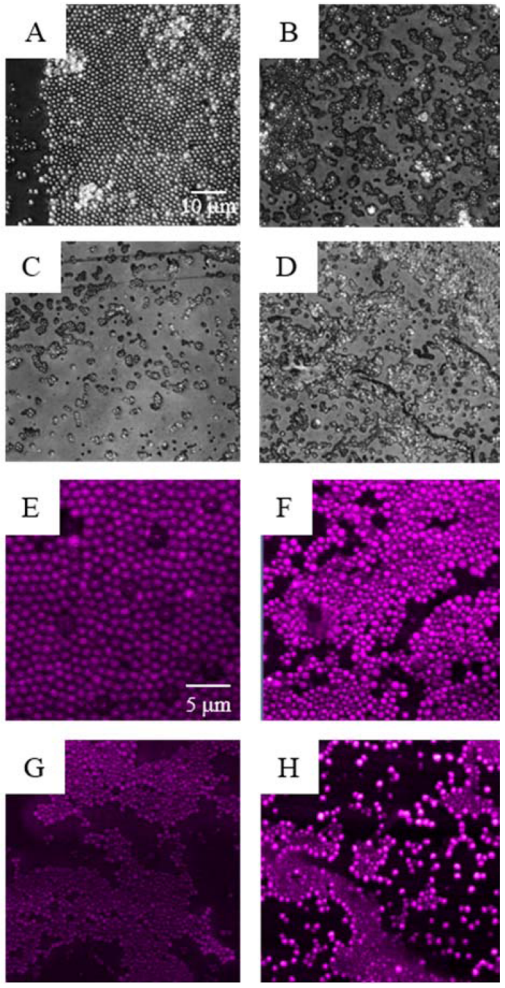

Figure 7. Optical and confocal fluorescent micrographs of (A and E) PSL-1, (B and F) PSL-6, (C and G) PSL-9, and (D and H) PSL-24 collected from prepared glass slide samples. The scale bars in A and E correspond to all of the optical and confocal images, respectively. Note the brightness and contrast of the confocal images were modified for visualization purposes.

Large Batch Synthesis. On the basis of the DOE analysis, necessary quantities for each component utilized for synthesis of the KR620-doped PSLs were identified. Using these conditions (see Experimental Section), a 2 L batch of PSLs, at 9 wt % organic material, was synthesized. The resultant mean particle diameter, predicted to be 1.06 ± 0.28 μm, was determined to be 0.87 ± 0.31 μm. The particle size distribution appeared to be bimodal with one distribution of PSLs centered at approximately 0.6 μm and another distribution centered at approximately 1.1 μm (see Supporting Information, Figure S1). As there is a significant mass difference in these two particle distributions, the majority of the particle mass was represented by the larger diameter distribution indicating that, although the population of the lower diameter population was significant, these reaction conditions favored the larger particle size mode. Since the airflow visualization experiments will be insensitive to a majority of the PSLs in the smaller diameter distribution, the effective standard deviation of the detected particle size was significantly lower than 0.31 μm.

Flow Measurement Demonstration. The flow and PIV instrumentation discussed above were used for comparison of Mie scattering and fluorescence imaging of the particles. For these tests, the lens aperture for the fluorescent camera was set at f/4, while the aperture for the Mie camera was set at f/22 (attenuating the signal by a factor of about 30 compared to the fluorescent camera) due to the brighter Mie signal. The resulting raw images are shown in Figure 8. As can be seen, there was considerable laser flare in the Mie-scattering image near the plate surface. Additionally, reflections from other objects in the test section appeared in the free streamflow, which drastically reduced the signal-to-noise ratio (SNR) of the images and impeded particle tracking. It is important to note that the collected Mie-scattering images represented a "worst-case scenario." Typically, several techniques would have been implemented to reduce laser flare, reflections, and other anomalies. None of these techniques were utilized in this work in order to ascertain the differences between the Mie-scattered and fluorescent emission signals. The bottom-left panel of Figure 8 shows that the use of fluorescent particles with an optical filter that blocks the laser's wavelength completely eliminated this laser flare. The plate surface was visible in the fluorescent images due to a combination of Raman scattering off of the aluminum and particles attached to the surface. However, this signal was low and did not leak onto neighboring pixels away from the plate surface and therefore did not decrease the SNR of the particles in the flow.

When these images were processed to obtain velocity vectors, the differences were clear. Figure 8 displays the average streamwise velocity vectors of 2000 images from each technique. The detrimental effects of reflections and laser flare

DOI: 10.1021/acsami.5b05584
ACS Appl. Mater. Interfaces 2015, 7, 20714−20725

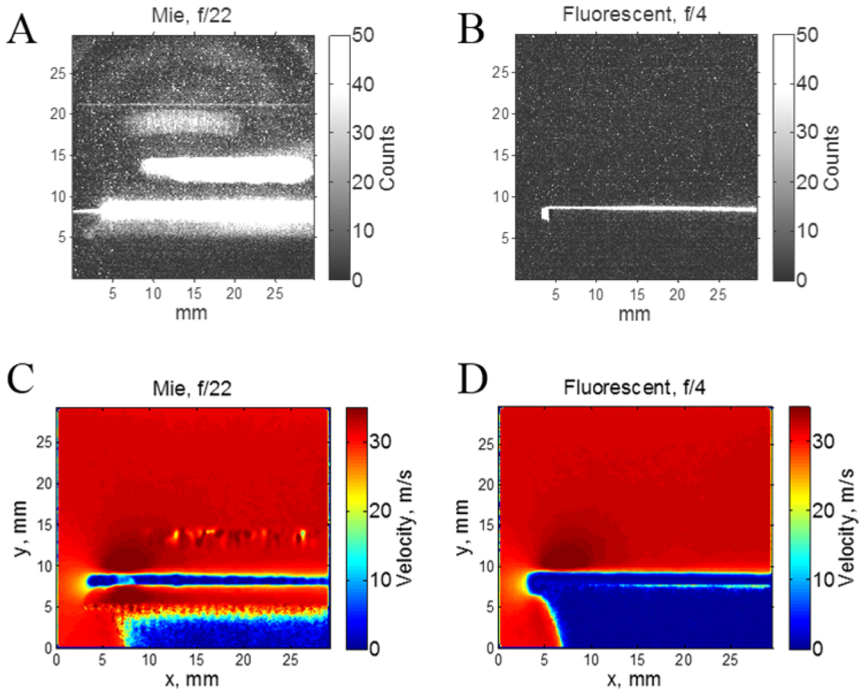

Figure 8. PIV with flat plate raw images for Mie-scattering (A) and fluorescent light (B) for the region of flow above the plate. Corresponding average streamwise velocity contours from the Mie-scattering (C) and fluorescent light (D) data.

can be clearly seen in the Mie images, both in the free stream and near the surface of the plate, where velocities were erroneously calculated to be over 10 m/s through the plate surface. The fluorescent data did not show such effects and gave an accurate measurement of the flow, approaching zero at the surface as expected. These tests demonstrated successful fluorescence imaging and PIV processing of the KR620-doped PSL particles in an airflow over 30 m/s, a first for fluorescent dye-doped PSL particles.

4. CONCLUSION

In this work, combined efforts to modify PSLs to include a fluorescent dye, KR620, along with development of measurement capabilities demonstrate the potential to gain access to more information with respect to airflow properties, boundary layer interactions, etc. To retain the dye within the PSLs, electrostatic interactions were utilized via incorporation of anionic functionalities within the polymer matrix and utilization of a cationic polyelectrolyte. In combination, these species formed an electrostatic double layer that prevented the anionic dye from leaching out of the polymer matrix. Additionally, the use of a buffer was determined to be of significance to retain the fluorescent properties of the dye once embedded. The use of design of experiments enabled efficient exploration of the design space that would have otherwise been unmanageable due to the large number of experimental variables. Ultimately, an optimal composition was identified and utilized to synthesize a relatively large batch, approximately 2 L, of KR620-doped PSLs that were used to conduct laser-induced fluorimetry airflow measurements. The fluorescent response from these particles mitigated the compromise of near-wall data that is commonplace in flow visualization experiments and will likely yield further understanding of airflow behavior deeper in the boundary layer.

■ ASSOCIATED CONTENT

Supporting Information

The Supporting Information is available free of charge on the ACS Publications website at DOI: 10.1021/acsami.5b05584.

Table of actual quantities used for batchwise synthesis of PSLs and particle size distribution of the PSLs generated in the large batch synthesis (PDF)

■ AUTHOR INFORMATION

Corresponding Author

*E-mail: c.j.wohl@nasa.gov.

Notes

The authors declare no competing financial interest.

■ ACKNOWLEDGMENTS

This work was funded by the NASA Aeronautics Research Mission Directorate (ARMD) NASA Aeronautics Research Institute (NARI) through Phase 1 and Phase 2 Seedling Projects. We also wish to acknowledge the work of summer LARSS students Max Verkamp and Brian Koh who contributed to work leading up to the present study. The authors appreciate the help of Richard DeLoach from NASA Langley for assisting with the design of experiments test matrix.

■ REFERENCES

(1) Albrecht, H. E.; Borys, M.; Damaschke, N.; Tropea, C. *Laser Doppler and Phase Doppler Measurement Techniques*; Springer Verlag: Berlin, Germany, 2003.

(2) Adrian, R.; Westerweel, J. *Particle Image Velocimetry*; Cambridge University Press: New York, 2011.

(3) Drain, L. E. *The Laser Doppler Technique*; John Wiley and Sons Inc.: New York, 1980; p 252.

(4) Meyers, J. F. In *Generation of Particles and Seeding*, von Karman Institute for Fluid Dynamics, NASA Langley Research Center,

DOI: 10.1021/acsami.5b05584
ACS Appl. Mater. Interfaces 2015, 7, 20714−20725

Hampton, VA, June 10−14; NASA Langley Research Center, Hampton, VA,1991.
(5) Chennaoui, D.; Angarita-Jaimes, D.; Ormsby, M. P.; Angarita-Jaimes, N.; McGhee, E.; Towers, C. E.; Jones, A. C.; Towers, D. P. Optimization and Evaluation of Fluorescent Tracers for Flare Removal in Gas-Phase Particle Image Velocimetry. *Meas. Sci. Technol.* **2008**, *19* (11), 115403.
(6) Lilley, G. M. The Radiated Noise From Isotropic Turbulence With Applications To The Theory Of Jet Noise. *J. Sound Vibration* **1996**, *190* (3), 463−476.
(7) Goodwin, J. W.; Hearn, J.; Ho, C. C.; Ottewill, R. H. The Preparation and Characterization of Polymer Latices Formed in the Absence of Surface Active Agents. *Br. Polym. J.* **1973**, *5*, 347−362.
(8) Bamnolker, H.; Margel, S. Dispersion Polymerization of Styrene in Polar Solvents: Effect of Reaction Parameters on Microsphere Surface Composition and Surface Properties, Size and Size Distribution, and Molecular Weight. *J. Polym. Sci., Part A: Polym. Chem.* **1996**, *34*, 1857−1871.
(9) *Dispersion Polymerization in Organic Media*; Barrett, K. E. J., Ed.; John Wiley and Sons: London, 1975; p 322.
(10) Vanderhoff, J. W. Mechanism of Emulsion Polymerization. *J. Polym. Sci., Polym. Symp.* **1985**, *72*, 161−198.
(11) Beylerian, N. M.; Vardanyan, L. R.; Harutyunyan, R. S.; Vardanyan, R. L. Kinetics and Mechanism of Potassium Persulfate Decomposition in Aqueous Solutions Studied by a Gasometric Method. *Macromol. Chem. Phys.* **2002**, *203*, 212−218.
(12) Kolthoff, I. M.; Miller, I. K. The Chemistry of Persulfate. I. The Kinetics and Mechanism of the Decomposition of the Persulfate Ion in Aqueous Medium. *J. Am. Chem. Soc.* **1951**, *73*, 3055−3059.
(13) Oh, S.; Kim, K.; Lee, B. H.; Shim, S. E.; Choe, S. TEMPO-mediated Dispersion Polymerization of Styrene in the Presence of Camphorsulfonic Acid. *J. Polym. Sci., Part A: Polym. Chem.* **2006**, *44* (1), 62−68.
(14) Li, Z.; Cheng, H.; Han, C. Mechanism of Narrowly Dispersed Latex Formation in a Surfactant-Free Emulsion Polymerization of Styrene in Acetone-Water Mixture. *Macromolecules* **2012**, *45*, 3231−3239.
(15) Qi, H.; Hao, W.; Xu, H.; Zhang, J.; Wang, T. Synthesis of Large-sized Monodisperse Polystyrene Microspheres by Dispersion Polymerization with Dropwise Monomer Feeding Procedure. *Colloid Polym. Sci.* **2009**, *287*, 243−248.
(16) Wu, C. A Simple Model for the Structure of Spherical Microemulsions. *Macromolecules* **1994**, *27*, 298−299.
(17) Goodwin, J. W.; Ottewill, R. H.; Pelton, R.; Vianello, G.; Yates, D. E. Control of Particle Size in the Formation of Polymer Latices. *Br. Polym. J.* **1978**, *10*, 173−180.
(18) Mubarekyan, E.; Santore, M. Characterization of Polystyrene Latex Surface by the Adsorption of Rhodamine 6G. *Langmuir* **1998**, *14*, 1597−1603.
(19) Eckenrode, H. M.; Jen, S.-H.; Han, J.; yeh, A.-G.; Dai, H.-L. Adsorption of a Cationic Dye Molecule on Polystyrene Microspheres in Colloids: Effect of Surface Charge and Composition Probed by Second Harmonic Generation. *J. Phys. Chem. B* **2005**, *109*, 4646−4653.
(20) Braga, M.; Leite, C. A. P.; Galembeck, F. Hydrophobic Polymer Modification with Ionic Reagents: Polystyrene Staining with Water-Soluble Dyes. *Langmuir* **2003**, *19* (18), 7580−7586.
(21) Behnke, T.; Wurth, C.; Hoffman, K.; Hubner, M.; Panne, U.; Resch-Genger, U. Encapsulation of Hydrophobic Dyes in Polystyrene Micro- and Nanoparticles via Swelling Procedures. *J. Fluoresc.* **2011**, *21* (3), 937−944.
(22) Lee, J.-H.; Gomez, I. J.; Sitterle, V. B.; Meredith, J. C. Dye-Labeled Polystyrene Latex Microspheres Prepared via a Combined Swelling-Diffusion Technique. *J. Colloid Interface Sci.* **2011**, *363*, 137−144.
(23) Pan, X.; Ju, J.; Li, J.; Wu, D Poly(Styrene-Acrylamide-Acrylic Acid) Copolymer Fluorescent Microspheres with Improved Hydrophilicity: Preparation and Influence on Protein Immobilization. *High Perform. Polym.* **2011**, *23* (3), 255−262.
(24) Holzapfel, V.; Lorenz, M.; Weiss, C. K.; Schrezenmeier, H.; Landfester, K.; Mailander, V. Synthesis and Biomedical Applications of Functionalized Fluorescent and Magnetic Dual Reporter Nanoparticles as Obtained in the Miniemulsion Process. *J. Phys.: Condens. Matter* **2006**, *18*, S2581−S2594.
(25) Ando, K.; Kawaguchi, H. High-Performance Fluorescent Particles Prepared via Miniemulsion Polymerization. *J. Colloid Interface Sci.* **2005**, *285*, 619−626.
(26) Taniguchi, T.; Takeuchi, N.; Kobaru, S.; Nakahira, T. Preparation of Highly Monodisperse Fluorescent Polymer Particles by Miniemulsion Polymerization of Styrene with a Polymerizable Surfactant. *J. Colloid Interface Sci.* **2008**, *327*, 58−62.
(27) Danehy, P.; Tiemsin, P.; Wohl, C.; Verkamp, M.; Lowe, T.; Maesto, P.; Byun, G.; Simpson, R. *Fluorescence Doped Particles for Simultaneous Temperature and Velocity Imaging*; National Aeronautics and Space Administration, 2012, TM-2012-217768.
(28) Lowe, T.; Maesto, P.; Byun, G.; Simpson, R.; Danehy, P.; Tiemsin, P.; Wohl, C. Laser Velocimetry with Fluorescent Dye-doped Polystyrene Microspheres. *Opt. Lett.* **2013**, *38* (8), 1197−1199.
(29) International Agency for Research on Cancer (IARC) - *Summaries & Evaluations*; 1978, *16*, 221.
(30) Lovejoy, K. S.; Purdy, G. M.; Iyer, S.; Sanchez, T. C.; Robertson, A.; Koppisch, A. T.; Del Sesto, R. E. Tetraalkylphosphonium-Based Ionic Liquids for a Single-Step Dye Extraction/MALDI MS Analysis Platform. *Anal. Chem.* **2011**, *83*, 2921−2930.
(31) Kitamura, M.; Murakami, K.; Yamada, K.; Kawai, K.; Kunishima, M. Binding of Sulforhodamine B to Human Serum Albumin: A Spectroscopic Study. *Dyes Pigm.* **2013**, *99* (3), 588−593.
(32) Inukai, S.; Tanma, T.; Orihara, S.; Konno, M. A Simple Method for Producing Micron-Sized, Highly Monodisperse Polystyrene Particles in Aqueous Media: Effects of Impeller Speed on Particle Size Distribution. *Chem. Eng. Res. Des.* **2001**, *79* (A), 901−905.
(33) Anderson, M. J.; Whitcomb, P. J. *DOE Simplified: Practical Tools for Effective Experimentation*; CRC Press: Boca Raton, FL, 2007; p 255.
(34) Tiemsin, P.; Wohl, C. J. *Refined Synthesis and Characterization of Controlled Diameter, Narrow Size Distribution Microparticles for Aerospace Research Applications*; National Aeronautics and Space Administration, 2012, TM-2012−217591.
(35) Danehy, P. M.; Hires, D. V.; Johansen, C. T.; Bathel, B. F.; Jones, S. B.; Gragg, J. G.; Splinter, S. C. Quantitative Spectral Radiance Measurements in the HYMETS Arc Jet. In *50th AIAA Aerospace Sciences Meeting*, Nashville, TN, 2012; pp Paper AIAA-2012-856.
(36) Spectroscopic Information for Kiton Red 620. www.photonicsolutions.co.uk (accessed 05/15/2015).
(37) Coppeta, J.; Rogers, C. Dual Emission Laser Induced Fluorescence for Direct Planar Scalar Behavior Measurements. *Exp. Fluids* **1998**, *25*, 1−15.

DOI: 10.1021/acsami.5b05584
ACS Appl. Mater. Interfaces 2015, 7, 20714−20725